Mitaplatin, a potent fusion of cisplatin and the orphan drug dichloroacetate

Shanta Dhar[a] and Stephen J. Lippard[a,b,1]

[a]Department of Chemistry and [b]Koch Institute for Integrative Cancer Research, Massachusetts Institute of Technology, 77 Massachusetts Avenue, Cambridge, MA 02139

Contributed by Stephen J. Lippard, October 29, 2009 (sent for review August 30, 2009)

The unique glycolytic metabolism of most solid tumors, known as the Warburg effect, is associated with resistance to apoptosis that enables cancer cells to survive. Dichloroacetate (DCA) is an anticancer agent that can reverse the Warburg effect by inhibiting a key enzyme in cancer cells, pyruvate dehydrogenase kinase (PDK), that is required for the process. DCA is currently not approved for cancer treatment in the USA. Here, we present the synthesis, characterization, and anticancer properties of *c,t,c*-[Pt(NH$_3$)$_2$(O$_2$CHCl$_2$)$_2$Cl$_2$], mitaplatin, in which two DCA units are appended to the axial positions of a six-coordinate Pt(IV) center. The negative intracellular redox potential reduces the platinum to release cisplatin, a Pt(II) compound, and two equivalents of DCA. By a unique mechanism, mitaplatin thereby attacks both nuclear DNA with cisplatin and mitochondria with DCA selectively in cancer cells. The cytotoxicity of mitaplatin in a variety of cancer cell lines equals or exceeds that of all known Pt(IV) compounds and is comparable to that of cisplatin. Mitaplatin alters the mitochondrial membrane potential gradient ($\Delta\psi_m$) of cancer cells, promoting apoptosis by releasing cytochrome *c* and translocating apoptosis inducing factor from mitochondria to the nucleus. Cisplatin formed upon cellular reduction of mitaplatin enters the nucleus and targets DNA to form 1,2-intrastrand d(GpG) cross-links characteristic of its own potency as an anticancer drug. These properties of mitaplatin are manifest in its ability to selectively kill cancer cells cocultured with normal fibroblasts and to partially overcome cisplatin resistance.

cancer therapy | DNA damage | mitochondrion | platinum | Warburg effect

Normal cells typically use mitochondrial oxidative phosphorylation to metabolize glucose and switch over to glycolysis only when there is little or no oxygen, producing lactate as a byproduct. Cancer cells avidly consume glucose for energy by glycolysis to survive in the hypoxic environment of malignant lesions (1), a phenomenon known as the Warburg effect (2). The dependence of cancer cells on glycolysis comes not only from oxygen deprivation, but also partly from their inability to synthesize ATP in response to the mitochondrial membrane potential gradient ($\Delta\psi_m$) (3). This unique glucose metabolic pathway of cancer cells has identified the mitochondrion as a prime target for cancer therapy (4–7). In addition, cancer cells develop the ability to avoid apoptosis by various pathways that ignore the command to commit cellular suicide (8, 9). Compounds that trigger apoptosis through selective action on mitochondrial target sites of cancer cells bypass defective upstream mechanisms and trigger apoptosis in tumor cells that are otherwise resistant (10).

Dichloroacetate (DCA) is used in humans to treat lactic acidosis (11). DCA inhibits the activity of pyruvate dehydrogenase kinase (PDK), thereby stimulating the mitochondrial enzyme pyruvate dehydrogenase (PDH). When turned off, PDH no longer converts pyruvate to acetyl-CoA required for mitochondrial respiration and glucose-dependent oxidative phosphorylation (12). DCA thus shifts cellular metabolism from glycolysis to glucose oxidation, decreasing $\Delta\psi_m$ (13) and helping to open mitochondrial transition pores (MTPs). This metabolic switch facilitates translocation of proapoptotic mediators like cytochrome *c* (cyt c) and apoptosis inducing factor (AIF), both of which stimulate apoptosis. DCA thereby drives cancer cells to commit suicide by apoptosis (13). Unlike most other anticancer agents, DCA does not appear to have any deleterious effect on normal cells. DCA reverses mitochondrial changes in a wide range of cancers, making malignant cells more vulnerable to normal cell death programs (14). Being an orphan drug, DCA is both nonpatentable and readily available, but it is not yet approved for use in cancer therapy (15). There is substantial preclinical evidence from both in vitro and in vivo models that DCA might be useful to treat cancer in humans, and a translation to early-phase clinical trials would be of interest (16–18). Funding for such trials would be a challenge because DCA is a generic drug. However, because it withdraws cancer cells from a state of apoptosis resistance, DCA is an attractive sensitizer that could be given concurrently with chemotherapy or radiation therapy. Alternatively, a formulation could be synthesized that incorporates DCA.

Platinum(II) compounds are used in 50% of all cancer therapies (19). Among these, cisplatin, carboplatin, and oxaliplatin have Food and Drug Administration approval and are in the clinic worldwide (20, 21). The use of platinum(II) drugs, cisplatin in particular, to treat malignancies is limited because of side effects and acquired resistance (22). Resistance can emerge from failure to execute apoptosis despite initiation of the apoptotic cascade caused by either the predominance of anti-apoptotic factors or defects in downstream effectors. Cisplatin resistance in ovarian carcinoma cells is associated with a reduced apoptotic response (23). To overcome tumor cell resistance and toxicity to normal tissues, we have been exploring strategies to target platinum constructs to cancer cells. Our tactic has been to employ substitutionally inert platinum(IV) compounds (24), which serve as prodrugs and release clinically effective levels of platinum(II) compounds, such as cisplatin, following cellular uptake (25–27). Appropriately designed platinum(IV) complexes are less likely to be deactivated before reaching their cancer cell destination target. The activity of platinum(IV) complexes generally involves reduction with loss of the axial ligands, affording an active platinum(II) complex that readily binds to DNA. Satraplatin is one such Trojan horse platinum(IV) compound that is currently under investigation for the treatment of patients with advanced prostate cancer (28).

We therefore designed a Pt(IV) compound (mitaplatin, **1**) having two DCA moieties (Fig. 1) in the axial positions. We hypothesized that DCA released inside the cells by reduction of the platinum would simultaneously alter mitochondrial metabolism and deliver a dose of cisplatin (Fig. 1). Mitaplatin was thereby expected to have dual killing modes toward cancer cells, one in which cisplatin interacts with its key target, nuclear DNA, and the other, DCA released upon reduction, following a

Author contributions: S.D. and S.J.L. designed research; S.D. performed research; S.D. and S.J.L. analyzed data; and S.D. and S.J.L. wrote the paper.

The authors declare no conflict of interest.

[1]To whom correspondence should be addressed at: Department of Chemistry, Room 18–498, Massachusetts Institute of Technology, 77 Massachusetts Avenue, Cambridge, MA 02139-4307. E-mail: lippard@mit.edu.

This article contains supporting information online at www.pnas.org/cgi/content/full/0912276106/DCSupplemental.

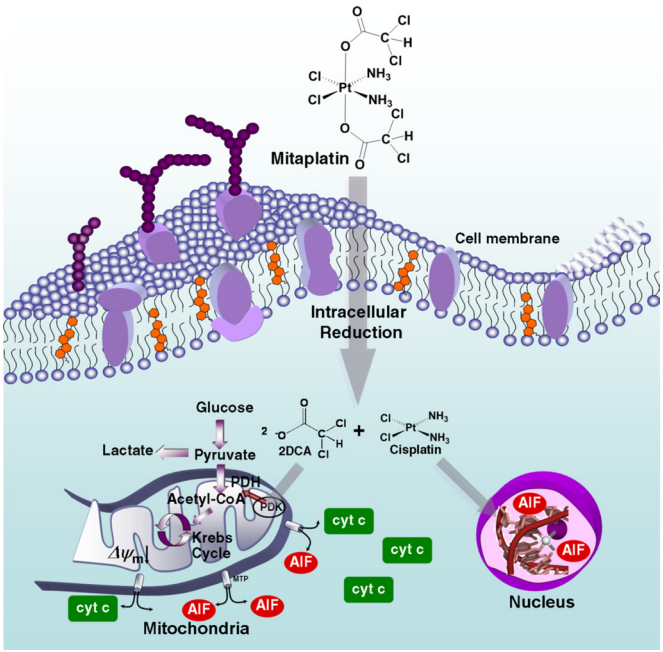

Fig. 1. Chemical structures and mechanism of action of mitaplatin (1). After crossing the plasma membrane, mitaplatin becomes reduced to release of the active drugs cisplatin and DCA. DCA inhibits mitochondrial PDK, which leads to PDH activation and increased glucose oxidation by promoting influx of acetyl-CoA into the mitochondria. DCA decreases the mitochondrial membrane potential ($\Delta\psi_m$). Opening of the $\Delta\psi_m$-sensitive mitochondrial transition pores (MTPs) leads to efflux of cyt c and AIF. Cisplatin formed in the reduction process interacts with its key target, nuclear DNA.

pathway to induce mitochondria-dependent apoptosis by mitochondrial membrane depolarization and efflux of proapoptotic mediators. Here, we describe the synthesis, characterization, and dual-action cell killing ability of mitaplatin as well as its remarkable ability to selectively destroy cancer cells in a coculture with normal fibroblasts.

Results and Discussion

Synthesis and Characterization of Mitaplatin (1). Mitaplatin (**1**), a formulation of DCA, was prepared by reaction of *c,c,t*-$[Pt(NH_3)_2Cl_2(OH)_2]$ with dichloroacetic anhydride in >50% yield. Its formation was evidenced by disappearance of the O–H stretching band of the starting compound and the presence of a C=O stretch at 1651 cm^{-1} in the infrared spectra. The structure was confirmed by ^1H, ^{13}C, and ^{195}Pt NMR spectroscopy, by HRMS, and by elemental analysis. ESI-HRMS (M–H) Calcd. = 554.8145, Found = 554.8138. ^1H NMR (DMSO-d_6) δ 7.95 (s, 2H), 6.52 (br, 6H); ^{13}C NMR (DMSO-d_6) δ 170.41, 65.27; ^{195}Pt NMR (DMSO-d_6): δ = 1205.28 ppm. Anal: Calcd for $C_4H_8Cl_6N_2O_4Pt$: C, 8.64; H, 1.45; N, 5.04. Found: C, 8.13; H, 1.65; N, 4.88. Mitaplatin is redox-active and displays an irreversible reduction revealed by cyclic voltammetric analysis. The Pt(IV)/Pt(II) couple is near −0.173 V vs. Ag/AgCl at pH 7.4 and the value at pH 6.0 is −0.152 vs. Ag/AgCl. Voltammograms are given in Figs. S1 and S2. These reduction potentials indicate that mitaplatin will be readily reduced in cells. The cathodic reduction potential depends on the electron-withdrawing power and the bulkiness of the axial and auxiliary ligands. The low reduction potential of mitaplatin is influenced by the presence of chlorine atoms from the DCA molecules near the platinum center (29).

In Vitro Cellular Cytotoxicity Assays. The ability of mitaplatin to promote cell death was evaluated by the MTT assay and the results were compared against those for cisplatin or DCA using

Table 1. Cell killing ability of mitaplatin

	IC_{50} (μM)		
Cell lines*	Cisplatin	Mitaplatin	DCA
NTera-2	0.043	0.051	>0.4
HeLa	1.2	2.0	>8.0
U2OS	3.9	6.4	>100
A549	12.0	14.0	>200
MCF-7	13.0	18.0	>100
MRC-5	9.5	18.3	>100
A2780	0.56	1.1	>120
A2780/CP70	6.0	3.34	>120

Comparison of IC_{50} values for mitaplatin, cisplatin, and DCA against cancer and normal cells as determined by the MTT assay.

*NTera-2, human testicular cancer; HeLa, human cervical cancer; U2OS, human osteosarcoma; A549, human lung carcinoma; MCF-7, human breast adenocarcinoma; MRC-5, normal lung fibroblast; A2780, human ovarian carcinoma; A2780/CP70, cisplatin-resistant human ovarian carcinoma.

NTera-2, HeLa, U2OS, A549, and MCF-7 cancer cells as well as MRC-5 normal fibroblasts (Fig. S3). Results are presented in Table 1. Mitaplatin has an IC_{50} value of 0.051 μM, comparable to that of cisplatin (IC_{50}, 0.043 μM), in cisplatin-sensitive testicular NTera-2 cells and is more toxic than DCA alone. In U2OS osteosarcoma cells, cisplatin has an IC_{50} of 3.9 μM, whereas that of mitaplatin is 6.4 μM. Similarly, in HeLa cervical cancer cells, comparable IC_{50} values for mitaplatin and cisplatin were observed, 2.0 and 1.20 μM, respectively. Control experiments with the well known platinum(IV) compound *c,c,t*-$[Pt(NH_3)_2Cl_2(O_2CCH_3)_2]$, revealed it to be several-fold less active than mitaplatin in all cells (Table S1). Mitaplatin was also established to have cytotoxicity comparable to that of cisplatin in the NCI/DTP 60 cell line growth inhibition assay, exceeding almost all known Pt(IV) compounds. This enhanced potency of mitaplatin is consistent with the expected dual killing mechanism.

Mitaplatin Promotes Apoptosis in Cancer Cells. To investigate the ability of mitaplatin to promote apoptosis in cancer cells by a mitochondrial-regulated mechanism, changes in the mitochondrial transmembrane potential ($\Delta\psi_m$) of cancerous NTera-2 and healthy normal fibroblast cells before and after mitaplatin treatment were investigated by two assays. Mitochondrial attack is associated with a drop in $\Delta\psi_m$. For this reason $\Delta\psi_m$ is an important parameter of mitochondrial function and has been used to monitor mitochondrial death. 5,5′,6,6′-Tetrachloro-1,1′,3,3′-tetraethylbenzimidazolylcarbocyanine iodide (JC-1) is a lipophilic cationic dye which, depending on $\Delta\psi_m$, accumulates as a green monomer in the cytoplasm or as red-emitting aggregates in hyperpolarized mitochondria of cancer cell (30). The negative charge established by the mitochondrial membrane potential allows the lipophilic dye, bearing a delocalized positive charge, to enter mitochondria where it accumulates. When a critical concentration is exceeded, J-aggregates form, which fluoresce red. In apoptotic cells, $\Delta\psi_m$ collapses, and JC-1 cannot accumulate in mitochondria. In these cells, JC-1 remains in the cytoplasm in a green fluorescent monomeric form. Control NTera-2 cells exhibited heterogeneous staining of the cytoplasm with both red and green fluorescence in the same cells (Fig. 2*A*). Treatment of these cells with mitaplatin for 4 h decreased the red fluorescence. Mitochondrial membrane depolarization was detected by a shift in fluorescence emission of JC-1 from red to green. There was no significant effect of mitaplatin on $\Delta\psi_m$ of normal fibroblasts or of cisplatin on $\Delta\psi_m$ of NTera-2 cells. The detailed results are given in Fig. S4.

To investigate whether DCA released from mitaplatin can restore the hyperpolarization of cancer cells to the level of normal

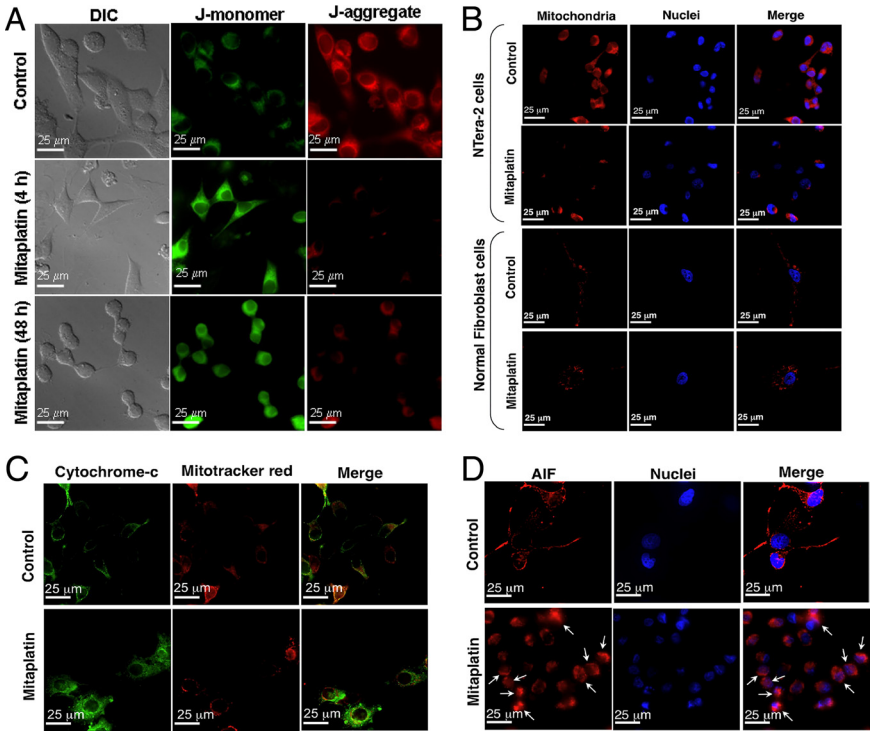

Fig. 2. Disruption of mitochondrial function and induction of apoptosis in cancer cells by mitaplatin. (*A*) Changes in the mitochondrial membrane potential as revealed by the JC-1 assay. Treatment with 100 μM mitaplatin dramatically caused the collapse of mitochondrial membrane potentials in NTera-2 cells. In live cells, JC-1 exists either as a green fluorescent monomer at depolarized membrane potentials (positive to −100 mV) or as an orange-red fluorescent J-aggregate at hyperpolarized membrane potentials (negative to −140 mV). The shift in membrane charge was observed by disappearance of fluorescent red-orange-stained mitochondria (large negative $\Delta\psi_m$) and an increase in fluorescent green-stained mitochondria (loss of $\Delta\psi_m$). (*B*) Reversal of mitochondrial membrane potential by tetramethyl rhodamine methyl ester (TMRM) assay. Mitaplatin significantly depolarized the NTera-2 cells but had no effect on the healthy normal fibroblast cells. Mitochondria were stained with mitotracker red. (*C*) Cytochrome c release visualized by fluorescence microscopy. Immunolocalization of cytochrome *c* (green) and mitochondrial morphology (red) shown in untreated NTera-2 cells and in mitaplatin treated NTera-2 cells. Cells were grown for 24 h on glass coverslips and treated with mitaplatin, fixed after treatment, and immunostained with anti-cytochrome *c* monoclonal antibodies. Mitochondria were stained with mitotracker red. (*D*) Translocation of AIF in mitaplatin treated cells. Staining of AIF (Ab) and nuclei (Hoechst) in NTera-2 cells before and after 12 h treatment with mitaplatin. Arrows indicate cells with particularly evident presence of AIF in the nucleus.

cells, we carried out a TMRM assay (31). All cancer cell lines have significantly more hyperpolarized $\Delta\psi_m$ compared to normal cells and therefore exhibit increased fluorescence of the $\Delta\psi_m$-sensitive positive dye tetramethyl rhodamine methyl ester, TMRM. Incubation of the NTera-2 cells with mitaplatin for 48 h reversed the hyperpolarization and returned the $\Delta\psi_m$ to the level of normal cells (Fig. 2*B*). In contrast, mitaplatin did not alter the $\Delta\psi_m$ of the normal fibroblasts. Because dichloroacetate activates pyruvate dehydrogenase, which increases delivery of pyruvate into mitochondria, DCA released upon reduction of mitaplatin (Fig. 1) increased glucose oxidation, depolarizing the mitochondria and returning the membrane potential to levels of the noncancer cells.

Mitochondrial cyt *c*, which functions as an electron carrier in the respiratory chain, translocates to the cytosol in cells undergoing apoptosis, where it participates in activation of apoptotic proteins (32). The mechanism responsible for this process is unknown. Cyt *c* release from mitochondria is an early event in the apoptotic process induced by mitaplatin treatment in NTera-2 cells, as visualized by using a FITC-conjugated antibody for the protein and fluorescence microscopy. The cytosol from untreated cells showed no detectable cyt *c* (Fig. 2*C*). In contrast, cytosolic cyt *c* accumulated significantly after 4 h of treatment with mitaplatin.

AIF is a proapoptotic mitochondrial protein (33). Like cyt *c*, AIF is a bifunctional protein having both electron transfer and apoptogenic functions. AIF is released from mitochondria and translocated to nuclei, stimulating chromatin condensation and DNA fragmentation. We were interested to determine whether mitochondrial outer membrane permeabilization by mitaplatin induces apoptosis only by release of caspase-dependent factors, such as cyt *c*, or whether caspase-independent processes, such as that mediated by AIF, might be operative. We therefore investigated the location of AIF in the mitaplatin-treated cells. As shown in Fig. 2*D*, mitaplatin treatment led to translocation of AIF from the mitochondria to nuclei of NTera-2 cells.

To quantify mitaplatin-induced apoptosis in cancer cells, an annexin-V assay was performed by using flow cytometry. With this analysis, we determined the percentage of apoptotic cells at 48 h after exposure to mitaplatin, cisplatin, or DCA. Apoptosis was detected in cancerous U2OS, HeLa, and A549 cells with 10 μM mitaplatin and cisplatin. Cisplatin at 10 μM concentration evoked apoptosis in normal MRC-5 cells whereas mitaplatin did not produce any detectable apoptosis with these normal cells (Table 2).

Visualization of Pt-1,2-d(GpG) Adduct Formation by Mitaplatin. Because the anticancer activity of cisplatin derives from the formation of intrastrand 1,2-d(GpG) cross-links on nuclear DNA (34), we investigated whether cisplatin released by reduction of mitaplatin leads to this signature event by using a monoclonal antibody R-C18 (35) specific for this adduct (*SI Text*). After 12 h incubation of NTera-2 cells with mitaplatin, formation of 1,2-d(GpG) intrastrand cross-links was observed by antibody-derived green fluorescence in the nuclei of these cells (Fig. S5). These results confirm that mitaplatin has dual cell-killing modes involving DCA, which destroys mitochondrial function, and

Table 2. Quantification of apoptosis induced by mitaplatin, cisplatin, and DCA using an annexin V assay

	HeLa		U2OS		A549		MRC5	
	Apoptosis, %	Necrosis, %	Apoptosis, %	Necrosis, %	Apoptosis, %	Necrosis, %	Apoptosis, %	Necrosis, %
Mitaplatin	57	10	37	63	55	1.0	2.8	0.2
Cisplatin	78	20	35	65	17.2	1.4	73.6	4.1
DCA	27	5.4	78	11.2	1.2	10.6	1.8	0.1

HeLa, human cervical cancer; U2OS, human osteosarcoma; A549, human lung carcinoma; MRC-5, normal lung fibroblast. [Mitaplatin], 10 μM, [Cisplatin], 10 μM, [DCA], 20 μM, incubation time 48 h.

cisplatin, which simultaneously impedes DNA-mediated processes in the nucleus.

Selective Killing of Cancer Cells by Mitaplatin. One of the main obstacles to cancer therapy is the inability to successfully target cancer cells, while not harming normal cells. Even when therapeutic agents are delivered locally to a primary tumor, systemic toxicities still arise. Modern medicine desperately needs anticancer molecules that kill cancer cells and leave healthy cells alone. Most cancer therapies today are very toxic to tumor and healthy cells alike, and the patient can succumb to treatment rather than the disease. Furthermore, cells develop a resistance to external agents, so chemotherapy may only work for a short time period. Because DCA has selective toxicity toward cancer cells by targeting PDK, we investigated whether mitaplatin would also display specificity for cancer. We therefore treated a coculture of normal fibroblasts and cancerous NTera-2 cells with mitaplatin, cisplatin, or a mixture of one equivalent of cisplatin and two equivalents of DCA, the stoichiometric composition released upon intracellular mitaplatin reduction. The morphology of these cells at different time points was examined by using bright field microscopy (Fig. 3*A*). The two types of cells in the coculture are clearly visible because of differences in their morphology. In the coculture, cisplatin and the mixture of cisplatin and DCA killed both the fibroblasts and NTera-2 cancer cells, whereas mitaplatin selectively killed the cancer cells. The results obtained in this study provide compelling evidence that mitaplatin can selectively kill cancer cells, leaving normal cells untouched.

To verify that preferential cancer cell killing occurs with mitaplatin, this study was further extended to a coculture of human lung cancer A549 cells and normal human lung fibroblasts MRC-5.

The selective killing of normal cells by mitaplatin was demonstrated by using a LIVE/DEAD viability assay, which allowed for the simultaneous determination of live and dead cells in a coculture by labeling live cells with calcein AM dye, which fluoresces only when cleaved by intracellular esterase enzymes, and ethidium heterodimer (EthD-1), which only enters dead cells with disrupted cell membranes (Fig. 3*B*). Fig. 3*B* confirms that, unlike cisplatin, a conventional chemotherapeutic agent, mitaplatin selectively induced cell death in human cancer A549 cells, but not in normal MRC-5 cells under the similar treatment conditions. To address whether the selective killing of cancer cells by mitaplatin might be a consequence of its selective uptake, we measured the nuclear and cytosolic concentrations of platinum by atomic absorption spectroscopy (AAS) after mitaplatin or cisplatin treatment of normal and cancer cells. Cytosolic and nuclear extracts were prepared from normal MRC-5 and cancerous A549 cells after incubation with 10 μM mitaplatin or cisplatin for 24 h. Platinum concentrations determined by AAS (Table S2) confirm the uptake of mitaplatin by both cells types.

Mitaplatin Action on Cisplatin-Resistant Cells. Although very little is known about the effects of cisplatin on the mitochondria of tumor cells (36), a recent study showed that it might have direct impact on mitochondria in head and neck cancer (37). Mitochondrial defects are associated with the cisplatin resistance phenotype (38), and several hypotheses have been suggested to explain this observation. A more negative membrane potential might promote translocation of the active, cationic form of cisplatin from the cytoplasm to mitochondria, thus diminishing platination of nuclear DNA. This effect would suggest that a combination of cisplatin with a mitochondrial targeting moiety would be an attractive therapeutic strategy for attacking cisplatin-resistant tumors. We therefore studied a pair of cisplatin sensitive A2780 and resistant A2780/CP70 ovarian cancer cells (Table 1 and Fig. S6). As controls we used cisplatin and *c*,*c*,*t*-[$Pt(NH_3)_2Cl_2(O_2CCH_3)_2$]. The cells displayed a low level of resistance to mitaplatin (IC_{50} for A2780, 1.1 μM; IC_{50} for A2780/CP70, 3.34 μM) compared to cisplatin (corresponding IC_{50} values of 0.56 and 6.0 μM). Results for the A2780/CP70 cells indicate that DCA plays a role in making cisplatin-resistant cells susceptible toward mitaplatin treatment. A2780/CP70 cells were

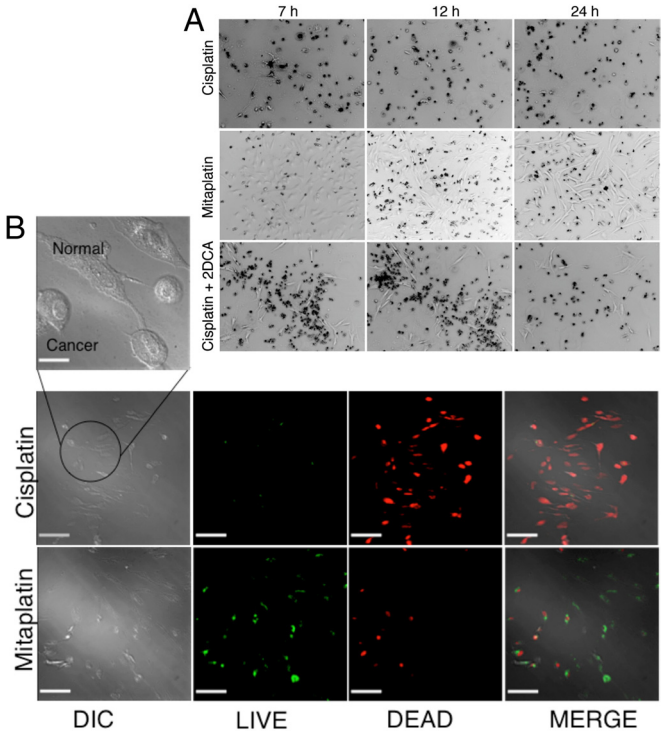

Fig. 3. Mitaplatin selectively induced apoptosis of human cancer cells and not normal cells. (*A*) Treatment of a coculture of normal fibroblast cells (elongated) and NTera-2 cells (round) with cisplatin, mitaplatin, and a mixture of one equivalent of cisplatin and two equivalents of DCA. (*B*) Selective killing of cancerous A549 (round) cells by mitaplatin in a coculture with normal MRC-5 (elongated) cells assayed using LIVE/DEAD staining. After mitaplatin or cisplatin exposure for 24 h, cells were stained with calcein AM (green fluorescence) and ethidium homodimer-1 (red fluorescence) to differentiate between live and dead cells, respectively.

much more resistant to the control platinum(IV) compound *c,c,t*-[$Pt(NH_3)_2Cl_2(O_2CCH_3)_2$]. These data suggest mitaplatin as a promising candidate for further development in the treatment of cisplatin-resistant cells.

Summary. In conclusion, mitaplatin displays a dual-killing mode that can only be effective in cancer cells. The platinum center interacts with its own target, nuclear DNA, and DCA released upon reduction attacks mitochondria. These results support the utility of mechanisms targeting cancer cell-specific pathways as an avenue for developing selective anticancer agents. Mitaplatin offers a formulation for future studies incorporating the orphan drug DCA to further its use in the clinic.

Materials and Methods

The complexes *cis*-[$Pt(NH_3)_2Cl_2$] (39) and *c,c,t*-[$Pt(NH_3)_2Cl_2(OH)_2$] (40) were synthesized as described. Distilled water was purified by passage through a Millipore Milli-Q Biocel water purification system (18.2 MΩ) containing a 0.22-μm filter. Anti-cytochrome *c* (Ab-1) sheep polyclonal antibody was procured from Calbiochem. Alexa Fluor 488-labeled secondary antibody donkey anti-(sheep IgG) was obtained from Invitrogen for cytochrome *c* detection. For AIF detection, we used a rabbit polyclonal IgG antibody from Santa Cruz Biotechnology, Inc. Alexa Fluor 546-labeled secondary antibody goat anti-(rabbit IgG) was purchased from Invitrogen. The detection of the cisplatin 1,2-d(GpG) intrastrand adduct was carried out using a monoclonal adduct-specific antibody R-C18 which was kindly provided by Jürgen Thomale (University of Duisburg-Essen). FITC labeled secondary antibody rabbit anti-(rat Ig) was obtained from Invitrogen. Specific adhesion slides for immunofluorescence were purchased from Squarix Biotechnology. JC-1 (5,5′,6,6′-tetrachloro-1,1′,3,3′ tetraethylbenzimidazolylcarbo-cyanine iodide) was obtained from Cayman Chemicals. ^{1}H, ^{13}C, and ^{195}Pt NMR spectra were recorded on a Bruker AVANCE-400 NMR spectrometer with a Spectro Spin superconducting magnet in the Massachusetts Institute of Technology Department of Chemistry Instrumentation Facility (MIT DCIF). Atomic absorption spectroscopic measurements were taken on a Perkin-Elmer AAnalyst 300 spectrometer. HRMS analysis was carried out on a Bruker Daltonics APEXIV 4.7 Tesla Fourier Transform Ion Cyclotron Resonance mass spectrometer in the MIT DCIF. Fluorescence imaging studies were performed with an Axiovert 200M inverted epifluorescence microscope (Zeiss) equipped with an EM-CCD digital camera C9100 (Hamamatsu). An X-Cite 120 metal-halide lamp (EXFO) was used as the light source. The microscope was operated with Volocity software (Improvision).

Synthesis of Mitaplatin c,c,t-[$Pt(NH_3)_2Cl_2(O_2CCHCl_2)_2$] (1). To a solution of *c,c,t*-[$Pt(NH_3)_2Cl_2(OH)_2$] (0.2 g, 0.6 mmol) in DMF (5 mL) was added dichloroacetic anhydride (0.28 g, 1.5 mmol) and the reaction mixture was stirred at room temperature for 4 h. Diethyl ether was added to the mixture to precipitate a light yellow solid, which was washed several times with diethyl ether and dried. Mitaplatin (**1**) was isolated in 55% (0.29 g) yield. IR (KBr): ν_{max} 3178, 3076, 3012, 1651, 1568, 1435, 1333, 1214, 1103, 1021, 819, 789, 723, 666, 582 cm^{-1}; ESI-HRMS (M–H) Calcd. = 554.8145, Found = 554.8138. ^{1}H NMR (DMSO-d_6) δ 7.95 (s, 2H), 6.52 (br, 6H); ^{13}C NMR (DMSO-d_6) δ 170.41, 65.27; ^{195}Pt NMR (DMSO-d_6): δ = 1205.28 ppm. Anal: Calcd for $C_4H_8Cl_6N_2O_4Pt$: C, 8.64; H, 1.45; N, 5.04. Found: C, 8.13; H, 1.65; N, 4.88.

Detection of Cyt *c* and AIF. NTera-2 cells were seeded on microscope coverslips (1 cm) at a confluence of 1,600 cells per slip and incubated overnight at 37 °C in DMEM. The medium was changed and mitaplatin was added to a final concentration of 100 μM. The cells were incubated for 4, 12, or 24 h at 37 °C. The medium was then removed and the cells were incubated with fixing solution for 1 h at room temperature followed by three washes with PBS (pH 7.4). Cells were then fixed with 4% paraformaldehyde in 0.1 M phosphate buffer (pH 7.4) at room temperature for 1 h, then washed twice with PBS. Cells were permeabilized with 0.1% Triton X-100 in PBS for 30 min, followed by six washes with PBS. Cells were then rinsed with blocking buffer (PBS, 0.1% goat serum, 0.075% glycin), incubated for 1 h at 37 °C with the anti-cytochrome *c* [anti-cytochrome *c* (Ab-1) sheep pAb, Calbiochem] antibody or AIF [AIF (H-300), Santa Cruz Biotechnology Inc.] antibody, both diluted 1:50 in blocking buffer, washed twice with blocking buffer, and incubated at 37 °C with Alexa Fluor 488 donkey anti-(sheep IgG) (Invitrogen) antibody for cyt *c* release and Alexa Fluor 546 goat anti-rabbit IgG (Invitrogen) antibody for AIF (dilution 1:50 in blocking buffer) for 1 h. After two washes with blocking buffer and four washes with water, Mitrotacker Red for cyt *c* release and Hoechst bis-benzamide for AIF release were used to stain mitochondria and nuclei, respectively. Microscope coverslips were mounted on microscope slides using mounting solution for imaging.

JC-1 Assay. GM61869 and NTera-2 cells were cultured on cover slips to a density of 1×10^6 cells/mL and incubated overnight at 37 °C. Cells were then treated with 100 μM mitaplatin for 4 and 48 h at 37 °C. A solution of JC-1 reagent (Cayman Chemicals; 10 μg/mL in DMEM) was added and incubation was carried out at 37 °C for 30 min. The cells were washed with PBS five times, fixed in 4% paraformaldehyde, and mounted onto glass slides using the procedure described above.

TMRM Assay. Analysis of mitochondrial membrane potential ($\Delta\psi_m$) was carried out by using TMRM. A similar procedure as mentioned above for the JC-1 assay was followed. Before fixing the cells, they were treated with 2 μM TMRM for 30 min at 37 °C.

LIVE/DEAD Assay. In vitro selective killing was performed using the LIVE/DEAD Viability/Cytoxicity Assay (Molecular Probes). A549 and MRC-5 cells were cultured on sterile glass coverslips as subconfluent monolayers for 24 h at 37 °C in 5% CO_2 and grown in DMEM supplemented with 10% FBS and 1% penicillin/streptomycin. The cells were then treated with 100 μM cisplatin or mitapltin for 24 h at 37 °C in 5% CO_2. The cells were washed with Dulbecco's PBS (D-PBS) to remove serum esterase activity generally present in serum-supplemented growth media before the assay. Calcein AM (4 mM in anhydrous dimethyl sulfoxide, DMSO) and EthD-1 (2 mM in DMSO/water, 1:4 vol/vol) were added to PBS (1:1,000 ratio) to produce a LIVE/DEAD working solution as recommended by the manufacturer. The samples were first washed in three changes of PBS and 100 μL LIVE/DEAD working solution was added on the coverslip and incubated at room temperature for 30 min. Subsequently, the samples were placed in PBS before being examined with a fluorescence microscope.

Annexin-V Assay. Flow cytometry with a Vybrant Apoptosis Assay kit (annexin V conjugated to allophycocyanin, Invitrogen) was used to determine whether treatment specifically induces apoptosis. Briefly, 5×10^5 cells for each cell line were seeded into six-well tissue culture plates and incubated overnight to 60–70% confluence under standard growth conditions. Media for the cell lines were then replaced with fresh growth media with and without a 10 μM dose of cisplatin, mitaplatin, and a 20 μM dose of DCA. Treatment groups for each cell line were replicated three times. The cells were then incubated for 48 h at 37 °C and harvested with 0.25% trypsin-EDTA. Cells were washed with PBS and subsequently stained by annexin V as per the manufacturer's protocol. Flow cytometry was performed on a BD LSR II flow cytometer (BD Biosciences) and data were analyzed on BD FACSDiva (BD Biosciences).

ACKNOWLEDGMENTS. This work was supported by the National Cancer Institute Grant CA034992 (to S.J.L.) and the Koch Institute for Integrative Cancer Research (S.D.).

1. Gatenby RA, Gillies RJ (2004) Why do cancers have high aerobic glycolysis? *Nat Rev Cancer* 4:891–899.
2. Warburg O (1956) On the origin of cancer cells. *Science* 123:309–314.
3. Samudio I, Fiegl M, Andreeff M (2009) Mitochondrial uncoupling and the Warburg effect: Molecular basis for the reprogramming of cancer cell metabolism. *Cancer Res* 69:2163–2166.
4. Larsson N-G, Luft R (1999) Revolution in mitochondrial medicine. *FEBS Lett* 455:199–202.
5. Schon EA, DiMauro S (2003) Medicinal and genetic approaches to the treatment of mitochondrial disease. *Curr Med Chem* 10:2523–2533.
6. Don AS, Hogg PJ (2004) Mitochondria as cancer drug targets. *Trends Mol Med* 10:372–378.
7. Spierings D, et al. (2005) Connected to death: The (unexpurgated) mitochondrial pathway of apoptosis. *Science* 310:66–67.
8. Hanahan D, Weinberg RA (2000) The hallmarks of cancer. *Cell* 100:57–70.
9. Kim J-W, Dang CV (2006) Cancer's molecular sweet tooth and the Warburg effect. *Cancer Res* 66:8927–8930.
10. Xu R-h, et al. (2005) Inhibition of glycolysis in cancer cells: A novel strategy to overcome drug resistance associated with mitochondrial respiratory defect and hypoxia. *Cancer Res* 65:613–621.
11. Stacpoole PW, et al. (2006) Controlled clinical trial of dichloroacetate for treatment of congenital lactic acidosis in children. *Pediatrics* 117:1519–1531.
12. Stacpoole PW, Nagaraja NV, Hutson AD (2003) Efficacy of dichloroacetate as a lactate-lowering drug. *J Clin Pharmacol* 43:683–691.
13. Bonnet S, et al. (2007) A mitochondria-K+ channel axis is suppressed in cancer and its normalization promotes apoptosis and inhibits cancer growth. *Cancer Cell* 11:37–51.

14. Stacpoole PW (1989) The pharmacology of dichloroacetate. *Metab Clin Exp* 38:1124–1144.
15. Pearson H (2007) Cancer patients opt for unapproved drug. *Nature* 446:474–475.
16. Cairns RA, Papandreou I, Sutphin PD, Denko NC (2007) Metabolic targeting of hypoxia and HIF1 in solid tumors can enhance cytotoxic chemotherapy. *Proc Natl Acad Sci USA* 104:9445–9450.
17. Cao W, et al. (2008) Dichloroacetate (DCA) sensitizes both wild-type and over expressing Bcl-2 prostate cancer cells in vitro to radiation. *Prostate* 68:1223–1231.
18. Wong JYY, Huggins GS, Debidda M, Munshi NC, De Vivo I (2008) Dichloroacetate induces apoptosis in endometrial cancer cells. *Gynecol Oncol* 109:394–402.
19. Galanski M, Jakupec MA, Keppler BK (2005) Update of the preclinical situation of anticancer platinum complexes: Novel design strategies and innovative analytical approaches. *Curr Med Chem* 12:2075–2094.
20. Rosenberg B, VanCamp L, Trosko JE, Mansour VH (1969) Platinum compounds: A new class of potent antitumor agents. *Nature* 222:385–386.
21. Wang D, Lippard SJ (2005) Cellular processing of platinum anticancer drugs. *Nat Rev Drug Discovery* 4:307–320.
22. Siddik ZH (2003) Cisplatin: Mode of cytotoxic action and molecular basis of resistance. *Oncogene* 22:7265–7279.
23. Perego P, et al. (1996) Association between cisplatin resistance and mutation of p53 gene and reduced Bax expression in ovarian carcinoma cell systems. *Cancer Res* 56:556–562.
24. Giandomenico CM, et al. (2002) Carboxylation of kinetically inert platinum(IV) hydroxy complexes. An entree into orally active platinum(IV) antitumor agents. *Inorg Chem* 34:1015–1021.
25. Dhar S, Gu FX, Langer R, Farokhzad OC, Lippard SJ (2008) Targeted delivery of cisplatin to prostate cancer cells by aptamer functionalized Pt(IV) prodrug-PLGA-PEG nanoparticles. *Proc Natl Acad Sci USA* 105:17356–17361.
26. Dhar S, Liu Z, Thomale J, Dai H, Lippard SJ (2008) Targeted single-wall carbon nanotube-mediated Pt(IV) prodrug delivery using folate as a homing device. *J Am Chem Soc* 130:11467–11476.
27. Mukhopadhyay S, et al. (2008) Conjugated platinum(IV)-peptide complexes for targeting angiogenic tumor vasculature. *Bioconjugate Chem* 19:39–49.
28. Choy H, Park C, Yao M (2008) Current status and future prospects for satraplatin, an oral platinum analogue. *Clin Cancer Res* 14:1633–1638.
29. Choi S, et al. (1998) Reduction and anticancer activity of platinum(IV) complexes. *Inorg Chem* 37:2500–2504.
30. Cossarizza A, Baccaranai-Contri M, Kalashnikova G, Franceschi C (1993) A new method for the cytofluorimetric analysis of mitochondrial membrane potential using the J-aggregate forming lipophilic cation 5,5′,6,6′-tetrachloro-1,1′,3,3′-tetraethylbenzimidazolcarbocyanine iodide (JC-1). *Biochem Biophys Res Commun* 197:40–45.
31. Floryk D, Houštěk J (1999) Tetramethyl rhodamine methyl ester (TMRM) is suitable for cytofluorometric measurements of mitochondrial membrane potential in cells treated with digitonin. *Biosci Rep* 19:27–34.
32. Jiang X, Wang X (2004) Cytochrome C-mediated apoptosis. *Annu Rev Biochem* 73:87–106.
33. Joza N, et al. (2001) Essential role of the mitochondrial apoptosis-inducing factor in programmed cell death. *Nature* 410:549–554.
34. Jamieson ER, Lippard SJ (1999) Structure, recognition, and processing of cisplatin-DNA adducts. *Chem Rev* 99:2467–2498.
35. Liedert B, Pluim D, Schellens J, Thomale J (2006) Adduct-specific monoclonal antibodies for the measurement of cisplatin-induced DNA lesions in individual cell nuclei. *Nucleic Acids Res* 34:e47.
36. Park SY, et al. (2004) Resistance of mitochondrial DNA-depleted cells against cell death: Role of mitochondrial superoxide dismutase. *J Biol Chem* 279:7512–7520.
37. Cullen KJ, Yang Z, Schumaker L, Guo Z (2007) Mitochondria as a critical target of the chemotheraputic agent cisplatin in head and neck cancer. *J Bioenerg Biomembr* 39:43–50.
38. Harper M-E, et al. (2002) Characterization of a novel metabolic strategy used by drug-resistant tumor cells. *FASEB J* 16:1550–1557.
39. Dhara SC (1970) A rapid method for the synthesis of *cis*-$[Pt(NH_3)_2Cl_2]$. *Indian J Chem* 8:193–194.
40. Hall MD, et al. (2003) The cellular distribution and oxidation state of platinum(II) and platinum(IV) antitumor complexes in cancer cells. *J Biol Inorg Chem* 8:726–732.